REPORT DOCUMENTATION PAGE

**AD-A271 047**

| 1. AGENCY USE ONLY (Leave blank) | 2. REPORT DATE | 3. REPORT TYPE AND DATES COVERED |
|---|---|---|

| 4. TITLE AND SUBTITLE | 5. FUNDING NUMBERS |
|---|---|
| Benchmark Calculations of Thermal Reaction Rates. 1. Quantal Scattering Theory | DAAL03-89-C-0038 |

**6. AUTHOR(S)**

David C. Chatfield, Donald G. Truhlar, and David W. Schwenke

| 7. PERFORMING ORGANIZATION NAME(S) AND ADDRESS(ES) | 8. PERFORMING ORGANIZATION REPORT NUMBER |
|---|---|
| University of Minnesota - School of Mathematics<br>127 Vincent Hall<br>Minneapolis, MN 55455 | |

| 9. SPONSORING/MONITORING AGENCY NAME(S) AND ADDRESS(ES) | 10. SPONSORING/MONITORING AGENCY REPORT NUMBER |
|---|---|
| U. S. Army Research Office<br>P. O. Box 12211<br>Research Triangle Park, NC 27709-2211 | ARO 27747.31-MA-CoE |

**11. SUPPLEMENTARY NOTES**

The view, opinions and/or findings contained in this report are those of the author(s) and should not be construed as an official Department of the Army position, policy, or decision, unless so designated by other documentation.

| 12a. DISTRIBUTION/AVAILABILITY STATEMENT | 12b. DISTRIBUTION CODE |
|---|---|
| Approved for public release; distribution unlimited. | |

DTIC
ELECTE
OCT 2 1 1993
S A D

**13. ABSTRACT (Maximum 200 words)**

The thermal rate coefficient for the prototype reaction $H + H_2 \rightarrow H_2 + H$ with zero total angular momentum is calculated by summing, averaging, and numerically integrating state-to-state reaction probabilities calculated by time-independent quantum-mechanical scattering theory. The results are very carefully converged with respect to all numerical parameters in order to provide high-precision benchmark results for confirming the accuracy of new methods and testing their efficiency.

**93-24887**

93 10 18 178

| 14. SUBJECT TERMS | 15. NUMBER OF PAGES |
|---|---|
| | 16. PRICE CODE |

| 17. SECURITY CLASSIFICATION OF REPORT | 18. SECURITY CLASSIFICATION OF THIS PAGE | 19. SECURITY CLASSIFICATION OF ABSTRACT | 20. LIMITATION OF ABSTRACT |
|---|---|---|---|
| UNCLASSIFIED | UNCLASSIFIED | UNCLASSIFIED | UL |

# Benchmark calculations of thermal reaction rates.
# I. Quantal scattering theory

David C. Chatfield and Donald G. Truhlar
*Department of Chemistry and Supercomputer Institute, University of Minnesota, Minneapolis,
Minnesota 55455-0431*

David W. Schwenke
*NASA Ames Research Center, Mail Stop 230-3, Moffett Field, California 94035*

The thermal rate coefficient for the prototype reaction $H + H_2 \rightarrow H_2 + H$ with zero total
angular momentum is calculated by summing, averaging, and numerically integrating state-to-
state reaction probabilities calculated by time-independent quantum-mechanical scattering
theory. The results are very carefully converged with respect to all numerical parameters in
order to provide high-precision benchmark results for confirming the accuracy of new methods
and testing their efficiency.

## I. INTRODUCTION

Quantum-mechanical calculations of chemical reaction rates are currently practical only for simple systems,[1-5] but they can be used to test approximate methods that are more generally applicable. As new methods and approaches become available, it is useful to have a clearly documented benchmark that can be used for testing their accuracy and efficiency. It is the goal of this and the following paper[6] to calculate the converged quantum-dynamical rate coefficient for one well-defined prototype case by two entirely independent methods to provide such a benchmark. The case chosen for study is the reaction $H + H_2 \rightarrow H_2 + H$, where the atoms are treated as distinguishable, the total angular momentum is zero, and the potential-energy surface is given by a double many-body expansion presented[7] previously. The method used in this paper involves time-dependent scattering theory to compute full sets of state-to-state transition probabilities at a series of total energies, followed by summing over final states corresponding to reaction, and averaging over initial states and energies according to a Boltzmann distribution.

Section II presents the theoretical formulation. Section III describes the calculations and presents the benchmark results and convergence studies. Section IV gives a summarizing conclusion.

## II. THEORY

Since total angular momentum ($J$) is rigorously conserved, we can separately evaluate the contribution of binary collisions with each value of the total angular momentum to the thermal reaction rate coefficient. The $J = 0$ contribution to the rate coefficient at temperature $T$ may be written[8]

$$k^{J=0}(T) = \frac{1}{h\Phi^R} \int_0^\infty dE\, e^{-E/kT} N^0(E), \qquad (1)$$

where $E$ is the total energy, $k$ is Boltzmann's constant, $\Phi^R$ is the reactants' partition function per unit volume in the center-of-mass frame, and $N^J(E)$ is the cumulative reaction probability[9] (hereafter referred to as the CRP). The CRP is defined as the sum over all state-to-state ($n \rightarrow n'$) reactive

transition probabilities $P^J_{\alpha n \alpha' n'}(E)$ from a given initial chemical arrangement $\alpha$ to all final reactive chemical arrangements $\alpha'$:

$$N^J(E) = \sum_{\substack{\alpha' \neq 1 \\ n,n'}} P^J_{1 n \alpha' n'}(E), \qquad (2)$$

where $n$ denotes the collection of all initial quantum numbers (arrangement $\alpha$, vibration $v$, rotation $j$, and orbital $l$), and $n'$ denotes the set of final ones. (Note that $\alpha$ and $\alpha'$ are also specified explicitly, although they are contained in $n$ and $n'$, respectively.)

## III. CALCULATIONS AND CONVERGENCE STUDIES
### A. Calculations

Converged quantum-dynamics calculations were carried out using a double many-body expansion[7] of the potential-energy surface. The high accuracy of this energy surface has recently been verified by new state-of-the-art electronic structure calculations.[10] The quantum-dynamics calculations were carried out by the generalized Newton variational principle for the $T$ matrix involving a Lebesgue square integrable ($\mathcal{L}^2$) expansion of the reactive amplitude density.[11,12] A formulation in terms of the $T$ matrix with complex boundary conditions for the distorted-wave radial functions and the radial Green's functions was used. Details of the basis sets and numerical procedures for this kind of calculation are given elsewhere,[12,13] and the parameters used for the present study are based on previous determinations[14] of converged parameters for state-to-state transition probabilities for this reaction.

We carried out calculations for $J = 0$ at 262 total energies in the range 0.27–1.66 eV. Equation (1) for $k^0$ was evaluated by fitting the calculated values of $N^0(E)$ with cubic splines and using repeated Gauss–Legendre quadrature to perform the integration. Plots of $e^{-E/kT} N^0(E)$ for 200, 600, and 1000 K, shown in Fig. 1, exhibit the shape typical of a thermal distribution of reactive collisions. The prominent shoulder in the 1000 K plot is due to a marked step-like

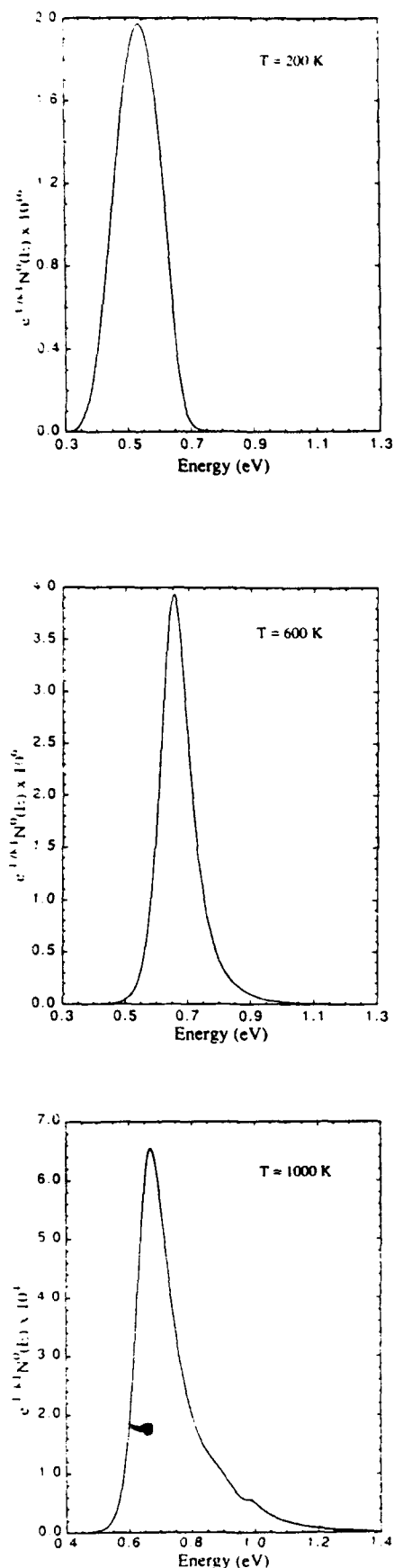Chatfield, Truhlar, and Schwenke: Thermal reaction rates. I

2041



FIG. 1. Boltzmann-weighted cumulative reaction probability for $J = 0$. (a) 200 K; (b) 600 K; (c) 1000 K.

feature in the CRP at 0.978 eV, which has been related to the threshold of a linear triatomic quantized transition state.[15]

The partition function $\Phi^R$ for distinguishable-atom $H_2$ without nuclear spin is given by the expression

$$\Phi^R = \left(\frac{2\pi\mu \bar{k}T}{h^2}\right)^{3/2} \sum_{v,j}(2j+1)e^{-\epsilon_{v,j}/kT}, \tag{3}$$

where $\mu$ is the reduced mass, $h$ is Plank's constant, and $\epsilon_{v,j}$ is the vibrational–rotational energy of the reactant $H_2$ diatom. The conversion factor used to convert from atomic units to $cm^3$ molecule$^{-1}$ s$^{-1}$ is 6.126 17. The rate constants for eight temperatures in the range 200–1000 K, calculated according to Eq. (1), are reported in Table I.

## B. Convergence studies

A careful analysis was performed to determine the limits of accuracy in the rate constants shown in Table I. There are three possible sources of error associated with the calculation: (i) convergence of the quantum-dynamical calculations, (ii) numerical integration of the Boltzmann-weighted CRP, and (iii) truncation of the integral in Eq. (1) to the energy range over which quantal calculations were performed. The estimated possible error associated with these sources is summarized in Table II. The rest of this section describes how we obtained these error estimates.

The first source of error is from convergence of the quantal results. This was evaluated by performing calculations with three different parameter sets, shown in Table III. A detailed explanation of most of the parameters in Table III can be found elsewhere.[12,13] Five of the parameters listed in Table III have not been discussed fully in previous publications. These are the screening parameters IEPSTS, IEPSRD, IEPSBS, IEPSWM, and IEPSBM which simplify the reactive scattering calculation by allowing certain quantities to be set to precisely zero when their magnitude is very small. Background discussion pertaining to the explanations of these parameters is given in Ref. 12; a detailed explanation follows here.

(1) The minimum bond distance for which the vibrational wave function with the highest value of $v$ and $j = 0$ exceeds $10^{-\text{IEPSTS}}$, and the maximum bond distance for which the vibrational wave function with the highest value of $j$ and the highest $v$ for that $j$ exceeds $10^{-\text{IEPSTS}}$ are determined. In calculating interarrangement ($\alpha \neq \alpha'$) integrals of the coupling potential, angles between the Jacobi translational coordinates $R_\alpha$ and $R_{\alpha'}$ that correspond to vibrational distances outside this range are excluded from the inner an-

TABLE I. Rate constants in $cm^3$ molecule$^{-1}$ s$^{-1}$.

| $T$ (K) | $k^a$ |
|---|---|
| 200 | $6.428 \times 10^{-20}$ |
| 300 | $8.505 \times 10^{-18}$ |
| 400 | $1.291 \times 10^{-16}$ |
| 600 | $1.988 \times 10^{-15}$ |
| 700 | $4.250 \times 10^{-15}$ |
| 1000 | $1.578 \times 10^{-14}$ |

TABLE II. Percent error in $k''$.

| Source of error | 200 K | 300 K | 400 K | 600 K | 700 K | 1000 K |
|---|---|---|---|---|---|---|
| Convergence of quantal CRPs | 0.028[a] | 0.024 | 0.024 | 0.022 | 0.022 | 0.021 |
| Point density | 0.0059 | 0.0027 | 0.0029 | 0.0025 | 0.0029 | 0.0034 |
| Truncation of integral | 0 | 0 | 0 | 0 | 0 | 0.0071 |
| Total | 0.034 | 0.027 | 0.027 | 0.025 | 0.025 | 0.032 |

[a] This should be interpreted as a relative error of $2.8 \times 10^{-4}$, i.e., $2.8 \times 10^{-2}\%$.

gular quadrature loop. If this procedure yields a negative value for the minimum, 0 is used instead.

(2) In performing quadratures at small values of the Jacobi translational coordinate, only distances for which all radial functions (of the regular solutions to the distortion potential problem and of the half-integrated Green's functions[12]) have magnitudes greater than $10^{-IEPSRD}$ times their maximum value are included in the integrals.

(3) When Gaussians are used for the translational basis, as is the case here, they are set to precisely 0 when their value falls below $10^{-IEPSBS}$ times their maximum value.

(4) Only values of $R_\alpha$ and $R_{\alpha+1}$ for which at least one matrix element of $W^{12}$ has magnitude greater than $10^{-IEPSWM}$ are included in the exchange integral.

(5) Only values of $R_\alpha$ and $R_\alpha + 1$ for which at least one matrix element of $\mathcal{B}^{12}$ has magnitude greater than $10^{-IEPSBM}$ are included in the exchange integral.

Set $A$ in Table III is the parameter set used to calculate

TABLE III. Sets of parameter values for GNVP calculations.

| Parameter | Explanation | Set A | Set B | Set C |
|---|---|---|---|---|
| $j_{max}$ $(v=0)$ | a | 13 | 14 | b |
| $j_{max}$ $(v=1)$ | a | 12 | 13 | b |
| $j_{max}$ $(v=2)$ | a | 11 | 12 | b |
| $j_{max}$ $(v=3)$ | a | 11 | 12 | b |
| $j_{max}$ $(v=4)$ | a | 10 | 11 | b |
| $j_{max}$ $(v=5)$ | a | ··· | 8 | ··· |
| $m$ | a | 10 | 12 | b |
| $R_1^G$ (a.u.) | a | 2.047 | 1.880 | b |
| $\Delta$ (a.u.) | a | 0.335 | 0.325 | b |
| $R_m''$ (a.u.) | a | 5.062 | 5.455 | b |
| $c$ | a | 1.4 | 1.3 | b |
| N(HO) | a | 75 | 90 | b |
| $R_{r,1}$ (a.u.) | a | 0.336 | 0.325 | 0.226 |
| $R_{r,N(F)}$ (a.u.) | a | 12.909 | 13.100 | 15.490 |
| $N_{tr}^{Qt}$ | a | 10 | 12 | b |
| $N_{tr}^{Qi}$ | a | 60 | 70 | b |
| $N_{tr}^{Qf}$ | a | 60 | 70 | b |
| $N^{QGL}$ | a | 12 | 13 | b |
| $N^{QR}$ | a | 14 | 15 | b |
| IEPSTS | c | 9 | b | 20 |
| IEPSRD | c | 20 | b | 30 |
| IEPSBS | c | 20 | b | 30 |
| IEPSWM | c | 20 | b | 30 |
| IEPSBM | c | 20 | b | 30 |

[a] See Refs. 12 and 13 for an explanation of these parameters.
[b] Same as for set $A$.
[c] See Sec. III B for an explanation of these parameters.

the CRPs. Set $B$ constitutes an increase with respect to set $A$ in the orders of quadratures, the size of the basis set, the range and overlap of the basis functions, and the range and grid point density of the finite difference grid. In set $C$ we varied the parameters not varied in set $B$, and two of the parameters which were varied only minimal amounts in set $B$ are varied more significantly.

The difference in the CRPs calculated with parameter sets $A$ and $B$ is shown as a function of energy in Fig. 2. For the range of energies which contributes significantly to the rate constant for the temperatures studied here ($E < 1.2$ eV), the differences in the values of $N^0(E)$ calculated with the two parameter sets are very small, less than 0.04%. Error in the quantum-dynamical calculations was parametrized with the straight lines shown in the figure, which constitute an estimate of the error in the CRP calculated with parameter set $A$. In order to represent a bound on the error in $k^0$ due to lack of convergence in the quantal calculations, a value for the rate constant was calculated with all of the CRPs increased by an amount corresponding to the linear parametrization of error in Fig. 2. The difference between the original and the recalculated rate constants, shown in Table II, is less than or equal to 0.028% for all temperatures studied.

The parameters varied in set $C$ have less effect on the results, and we can illustrate this by considering the same set of energies for which sets $A$ and $B$ were compared. The largest error in the CRP calculated with set $C$ relative to that
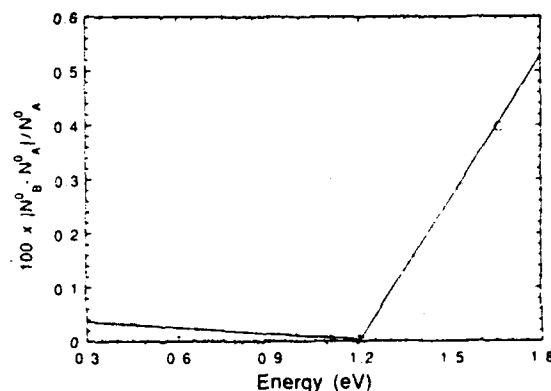


FIG. 2. Relative percent difference in the CRP as calculated with the production parameter set $A$ and the convergence-check parameter set $B$. The circles are data points, and the straight lines represent the parametrization used to estimate the possible error in $k''$ due to error in the quantal CRPs caused by the parameters varied in set $B$.

calculated with set $A$ is $3 \times 10^{-2}\%$ (at 0.4 eV), and there is no correlation of larger errors with higher energies (the error at 1.66 eV is only $5 \times 10^{-4}\%$). Thus the calculations performed with set $A$ are extremely well converged with respect to the parameters varied in set $C$.

The second source of error is that associated with the numerical integration of the Boltzmann-weighted CRP because the number of data points is finite. In order to evaluate this source of error, we calculated the effect on the rate constant of using only subsets of the full set of 262 energies in the calculation. To do this, we omitted one of every three energies in the full data set. Since the cubic spline fit is expected to be more sensitive to the omission of a data point at a region of high curvature in the function $e^{-E/kT}N^0(E)$, the points to be omitted were chosen in three different ways in order to provide a comprehensive view of their effect. In particular, every third point was omitted beginning with either the first, the second, or the third point. The relative difference between the rate constant calculated with points omitted and that calculated with the full data set is less than or equal to 0.0059% for all temperatures studied, as reported in Table II (the error reported for each temperature is the largest of the three differences obtained by the above procedure).

The third source of error is the finite upper bound of the integration. This was studied by truncating the integration at a smaller upper bound and comparing it to the results obtained with the full energy range of 0.27–1.66 eV (since the zero-point energy of the $H_2$ vibrational motion is 0.27 eV, the CRP is nonzero only at energies greater than 0.27 eV, and this energy can be used as the lower bound for the integration without causing truncation error). The relative error in the rate constant is insensitive (to six decimal places) to the upper bound of the integration until the temperature exceeds 700 K. An estimate of the error was made by approximating $N^0(E)$ as a linear function at energies above 1.66 eV (see Fig. 3) based on an appropriate fit to the envelope of the oscillatory $N^0(E)$ in the range 1.4–1.66 eV. The possible error in the rate constant is then equated to the integral of the product of the linear function and the appropriate Boltzmann-weighting factor from 1.66 eV to infinity. The

error thus calculated is less than $10^{-4}\%$ for $T \leqslant 700$ K, and is $7 \times 10^{-3}\%$ at 1000 K.

Finally, an upper bound on the total possible error in the rate constant was estimated by summing the individual error estimates. As can be seen in Table II, the total error for all of the temperatures studied is less than or equal to 0.034%. Thus these values should serve as definitive benchmarks for testing new and/or approximate procedures. One such use, checking the stability of results obtained by a time-dependent theoretical method, the flux autocorrelation method,[6,8,16] is presented in the following article. As we shall see,[6] the two calculations differ by at most 0.022% for the temperatures common to both studies. This value is well within the tolerances for the calculations reported here and suggests that these tolerances are generous. The excellent agreement confirms the accuracy of both calculations, since the methods used are *completely* different.

## IV. CONCLUSION

The distinguishable-atom rate constant for the reaction $H + H_2 \rightarrow H_2 + H$, where the total angular momentum is zero, was calculated by a method that is exact to within the limits imposed by the Born–Oppenheimer approximation and the best available potential-energy surface, the double-many-body-expansion potential-energy function of Ref. 7. Careful analysis places an estimated bound on the error in these results of at most 0.034% for temperatures in the range 200–1000 K. Agreement with rate constants calculated[6] by the flux autocorrelation method to within these tolerances confirms the accuracy of both calculations.

[1] G. C. Schatz and A. Kuppermann. J. Chem. Phys. **65**, 4668 (1976).
[2] B. C. Garrett, D. G. Truhlar, and G. C. Schatz, J. Am. Chem. Soc. **108**, 2876 (1986).
[3] D. C. Clary, J. Chem. Phys. **83**, 1685 (1985); G. C. Lynch, D. G. Truhlar, and B. C. Garrett, *ibid.* **90**, 3102 (1989).
[4] J. Z. H. Zhang and W. H. Miller, J. Chem. Phys. **91**, 1528 (1989).
[5] T. J. Park and J. C. Light, J. Chem. Phys. **91**, 974 (1989).
[6] P. N. Day and D. G. Truhlar, following paper, J. Chem. Phys. **94**, 2045 (1991).
[7] A. J. C. Varandas, F. B. Brown, C. A. Mead, D. G. Truhlar, and N. C. Blais, J. Chem. Phys. **86**, 6258 (1987).
[8] W. H. Miller, J. Chem. Phys. **61**, 1823 (1974).
[9] W. H. Miller, J. Chem. Phys. **62**, 1899 (1975). See also W. H. Miller, in *Potential Energy Surfaces and Dynamics Calculations*, edited by D. G. Truhlar (Plenum, New York, 1981), p. 265.
[10] C. W. Bauschlicher, S. R. Langhoff, and H. Partridge, Chem. Phys. Lett. **170**, 345 (1990).
[11] R. G. Newton, *Scattering Theory of Particles and Waves* (McGraw-Hill, New York, 1966). Sec. 11.3; G. Staszewska and D. G. Truhlar, Chem. Phys. Lett. **130**, 341 (1986), J. Chem. Phys. **86**, 2793 (1987); D. W. Schwenke, K. Haug, D. G. Truhlar, Y. Sun, J. Z. H. Zhang, and D. J. Kouri, J. Chem. Phys. **91**, 6080 (1987).
[12] D. W. Schwenke, K. Haug, M. Zhao, D. G. Truhlar, Y. Sun, J. Z. H. Zhang, and D. J. Kouri, J. Phys. Chem. **92**, 3202 (1988); D. W. Schwenke, M. Mladenovic, M. Zhao, D. G. Truhlar, Y. Sun, and D. J. Kouri, in *Supercomputer Algorithms for Reactivity, Dynamics and Kinet-
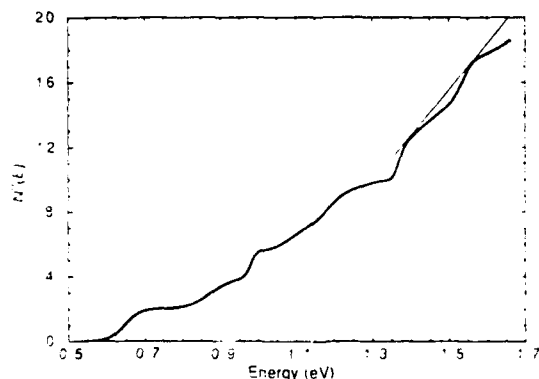
FIG. 3. Cumulative reaction probability for $J = 0$. The straight line is the linear approximation to $N^0(E)$ used to estimate the contribution to the rate constant from energies above 1.66 eV, the highest energy for which we calculated converged quantal results.

ics of Small Molecules, edited by A. Laganá (Kluwer, Dordrecht, 1989), p. 131; Y. Sun, C.-h. Yu, D. J. Kouri, D. W. Schwenke, P. Halvick, M. Mladenovic, and D. G. Truhlar. J. Chem. Phys. 91, 1643 (1989).

M. Zhao, M. Mladenovic, D. G. Truhlar, D. W. Schwenke, Y. Sun, D. J. Kouri, and N. C. Blais, J. Am. Chem. Soc. 111, 852 (1989).

M. Zhao, M. Mladenovic, D. G. Truhlar, D. W. Schwenke, O. Sharafed-

din, Y. Sun, and D. J. Kouri. J. Chem. Phys. 91, 5302 (1989).

D. C. Chatfield, R. S. Friedman, D. G. Truhlar, B. C. Garrett, and D. W. Schwenke, J. Am. Chem. Soc. (in press).

W. H. Miller, S. D. Schwartz, and J. W. Tromp, J. Chem. Soc. 79, 4889 (1983); J. W. Tromp and W. H. Miller, Faraday Discuss. Chem. Soc. 84, 441 (1987).

DTIC QUALITY INSPECTED 2

| Accesion For | |
|---|---|
| NTIS CRA&I | ☑ |
| DTIC TAB | ☐ |
| Unannounced | ☐ |
| Justification | |
| By | |
| Distribution / | |
| Availability Codes | |
| Dist | Avail and / or Special |
| A-1 | 20 |